Possible New Resonance from $W_L W_L$-hh Interchannel Coupling

Rafael L. Delgado, Antonio Dobado, and Felipe J. Llanes-Estrada

Física Teórica I, Universidad Complutense, Parque de las Ciencias 1, 28040 Madrid, Spain
(Received 21 August 2014; revised manuscript received 19 February 2015; published 4 June 2015)

We propose and theoretically study a possible new resonance caused by strong coupling between the Higgs-Higgs and the $W_L W_L$ ($Z_L Z_L$) scattering channels, without regard to the intensity of the elastic interaction in either channel at low energy (that could be weak as in the standard model). We expose this channel-coupling resonance from unitarity and dispersion relations encoded in the inverse amplitude method, applied to the electroweak chiral Lagrangian with a scalar Higgs boson.

The LHC experiments CMS and ATLAS [1] have seemingly found what looks like a Higgs boson (mainly an excess of four-lepton events and two-photon events at 125 GeV suggestive of scalar quantum numbers). This finding has been widely discussed, but less recognized is the equally interesting fact that no new physics beyond the standard model (SM) appears up to energies of 600–700 GeV for generic searches [2], as shown in Fig. 1. Therefore, the unknown system giving rise to the electroweak-symmetry breaking [the symmetry-breaking sector (SBS)] from $SU(2)_L \times U(1)_Y$ to $U(1)_{em}$ should contain four low-mass states: the three would-be Goldstone bosons ω^a ($a = 1, 2, 3$) responsible for the $W^\pm$ and Z masses and the recently discovered particle h. Because this Higgs-like boson turns out to be light and the spectrum is gapped, up to the scale of any new physics, it is natural to think of it also as an approximate (composite) Goldstone boson (GB) itself [3], for instance, as one of the GB corresponding to the spontaneous symmetry breaking from a group G to a group H with $\dim(G) - \dim(H) = 4$; this is the case of the so-called MCHM [minimal composite Higgs model [4], with $G = SO(5)$ and $H = SO(4)$]. Another exciting possibility is that the Higgs boson is a dilaton [5] (the Goldstone boson associated with spontaneous breaking of the scale symmetry of the SBS).

Assuming the approximate, well-established $SU(2)_{L+R}$ custodial symmetry, the low-energy GB dynamics can be properly described by a $SU(2)_L \times U(1)_Y$ gauged non-linear effective Lagrangian [6,7], which is an extension of the former Higgs-less electroweak chiral Lagrangian [8]. Thus, the three ω^a GB fields parametrize the coset $SU(2)_L \times SU(2)_R / SU(2)_{L+R}$, and the Higgs-like boson h is a custodial isospin singlet.

In this work, we are concerned with the $W_L W_L$, $Z_L Z_L$, and hh scattering. This is because, thanks to the equivalence theorem [9], we can get information about the unknown SBS of the SM by studying the GB dynamics, whose amplitudes approximate well those of the longitudinal vector bosons W_L and Z_L (W_L for short in the following) of the SM for energies well above the W mass

($E \gg M_W$). In this regime, we can also neglect the h boson mass, since $M_h = 125$ GeV $\sim M_W$. Then the relevant Lagrangian for $W_L W_L$ and hh scattering is [10]

$$
\mathcal{L} = \left(1 + 2a\frac{h}{v} + b\frac{h^2}{v^2}\right)\frac{\partial_\mu \omega^a \partial^\mu \omega^b}{2}\left(\delta^{ab} + \frac{\omega^a \omega^b}{v^2}\right)
$$
$$
+ \frac{4a_4}{v^4}(\partial_\mu \omega^a \partial_\nu \omega^a)^2 + \frac{4a_5}{v^4}(\partial_\mu \omega^a \partial^\mu \omega^a)^2
$$
$$
+ \frac{2d}{v^4}\partial_\mu h \partial^\mu h \partial_\nu \omega^a \partial^\nu \omega^a + \frac{2e}{v^4}(\partial_\mu h \partial^\mu \omega^a)^2
$$
$$
+ \frac{1}{2}\partial_\mu h \partial^\mu h + \frac{g}{v^4}(\partial_\mu h \partial^\mu h)^2, \tag{1}
$$

which should be valid for $M_W, M_h \ll E \ll 4\pi v \simeq 3$ TeV. Thus, we have set $M_h = M_W = M_Z \simeq 0$. Different SBS dynamics can be modeled by a proper tuning of the parameters a, b, a_4, a_5, d, e, and g. The last five of them must be renormalized to some scale μ to absorb the one-loop divergencies coming from the lowest order (LO), i.e., the first term in the Lagrangian, in a similar way as in the chiral perturbation theory [11]. In the SM, $a^2 = b = 1$ and the rest of the tree-level parameters vanish ($a_4 = a_5 = d = e = g = 0$). As is well known in this particular case, we get a linear theory which is renormalizable in the standard way and weakly interacting for light h.

From the Lagrangian density in Eq. (1), the LO partial waves with $I = J = 0$ (I being the custodial isospin) can be easily computed, and one finds
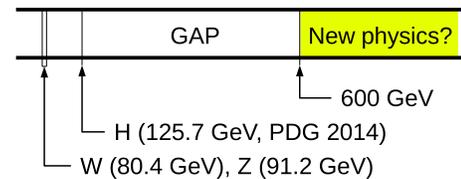

FIG. 1 (color online). Electroweak-symmetry-breaking sector of the standard model after LHC run I: there are four "low-energy" bosons and any new physics is split by a mass gap.

$$A_0(\omega\omega \to \omega\omega) = \frac{s}{16\pi v^2}(1 - a^2),$$

$$T_0(hh \to hh) = 0,$$

$$M_0(\omega\omega \to hh) = \frac{\sqrt{3}s}{32\pi v^2}(a^2 - b). \qquad (2)$$

From these low-energy theorems, we can expect strong $W_L W_L$ elastic scattering whenever $a^2 \neq 1$ [as Eq. (2) grows with $s = E_{cm}^2$]. For $b \neq a^2$ we have strong mixing between the $W_L W_L$ and hh channels [12,13] even in the case $a = 1$ (no LO contribution to $W_L W_L$ elastic scattering). As we will show below, this strong mixing gives rise to a new resonance in the $I = J = 0$ channel for an important region of the available (a, b) parameter space after taking into account the experimental information coming from the LHC. At next to leading order (NLO), all three amplitudes in Eq. (2) acquire one-loop contributions of the order of $O(s^2)$. The elastic ones A_1 and T_1 are accompanied by logarithmic left and right cuts (LC and RC, respectively) in the s plane, entailing an imaginary part for physical energy corresponding to s just above the RC. Those amplitudes have already been reported in the recent literature [10,14]. The divergences appearing for massless W and h can be absorbed by renormalization of the a_4, a_5, d, e, and g parameters, but no a or b renormalization is needed in this case.

In this work, we want to focus on the very interesting phenomenon of the strong mixing appearing whenever $a^2 \neq b$. In order to emphasize this point, we will concentrate first on the particular case where $a = 1$ (no direct $W_L W_L$ LO elastic scattering) and the rest of the parameters except b vanish [15]. As the renormalized parameters depend on the renormalization scale μ, that particularly simple choice requires one to set this scale to some given value that now plays the role of an ultraviolet cutoff. For definiteness, we will take $\mu = 4\pi v \simeq 3$ TeV, which is roughly the limit of applicability of our effective theory. The relevant NLO $I = J = 0$ partial waves read [10]

$$A_1(\omega\omega \to \omega\omega) = \frac{s^2(1 - b)^2}{256\pi^3 v^4}$$
$$\times \left[\frac{17}{9} - \frac{1}{6}\log\left(\frac{s}{\mu^2}\right) - \frac{3}{4}\log\left(\frac{-s}{\mu^2}\right)\right], \quad (3)$$

$$T_1(hh \to hh) = \frac{s^2(1 - b)^2}{32\pi^3 v^4}$$
$$\times \left[\frac{1}{3} - \frac{1}{16}\log\left(\frac{s}{\mu^2}\right) - \frac{3}{32}\log\left(\frac{-s}{\mu^2}\right)\right], \quad (4)$$

$$M_1(\omega\omega \to hh) = \frac{\sqrt{3}s^2(1 - b)^2}{9216\pi^3 v^4}\left[\frac{1}{2} - \log\left(\frac{s}{\mu^2}\right)\right]. \quad (5)$$

These partial waves have adequate analytical properties featuring a LC and also a RC just under the physical region

$s = E_{cm}^2 + i\epsilon$. However, unitarity is satisfied only perturbatively, with $\text{Im}A_1 = \text{Im}T_1 = |M_0|^2$ on the RC. Notice also that the cross-channel amplitude M_1 has only a LC and is thus purely real $[\text{Im}(M_0 + M_1) = 0]$ on the RC. As the amplitudes grow with s, they will eventually violate the unitarity bound (for example, $\text{Im}A \leq 1$). By grouping the two coupled channels in matrix form,

$$F = F_0 + F_1 + \cdots$$
$$= \begin{pmatrix} 0 & M_0 \\ M_0 & 0 \end{pmatrix} + \begin{pmatrix} A_0 & M_1 \\ M_1 & T_1 \end{pmatrix} + \cdots, \quad (6)$$

the perturbative unitarity relation satisfied is $\text{Im}F_1 = F_0^\dagger F_0$, but exact unitarity requires $\text{Im}F = F^\dagger F$ instead. However, there is a very well-known method, based on dispersion relations, called the inverse amplitude method (IAM) [16], that allows us to fully unitarize the perturbative partial waves, even in the coupled-channel case [17]. The resulting amplitudes are given by $F^{\text{IAM}} := F_0(F_0 - F_1)^{-1}F_0$. The IAM amplitudes still have the analytical properties found above, but now they fulfill exact unitarity. In addition, the determinant of $F_0 - F_1$ appearing in the denominators allows for the possibility of having poles in the second Riemann sheet for some regions of the parameter space. When they are close enough to the physical region, those poles have the natural interpretation of dynamical resonances. The IAM amplitudes have been extensively used to fit meson-meson scattering data [18]. The method has also been applied to $W_L W_L$ elastic scattering [19], where resonances were found in different channels in terms of the a_4 and a_5 parameters. In this work, we are rather interested in the pure coupled-channel resonances appearing even for $a = 1$. The IAM amplitudes are given in this case by

$$F^{\text{IAM}} = \frac{M_0^2}{(M_0 - M_1)^2 - A_1 T_1}\begin{pmatrix} A_1 & M_0 - M_1 \\ M_0 - M_1 & T_1 \end{pmatrix}, \quad (7)$$

whose perturbative expansion coincides with Eq. (6) at $O(s^2)$ but that satisfies exact unitarity, $\text{Im}F^{\text{IAM}} = (F^{\text{IAM}})^\dagger F^{\text{IAM}}$, as is easily checked. The IAM resums the imaginary parts of diagrams like that in Fig. 2.

In Fig. 3, we show the square moduli of two distinct matrix elements of F^{IAM} (A^{IAM} and M^{IAM}). For b nearly 1, the amplitude vanishes in the LHC region of interest (with $W_L W_L \to W_L W_L$ reducing to the small SM amplitude).
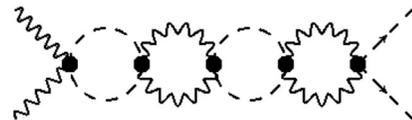

FIG. 2. Typical Feynman diagram mixing the $\omega\omega$ (wiggled lines) and the Higgs-Higgs (dashed lines) channels.
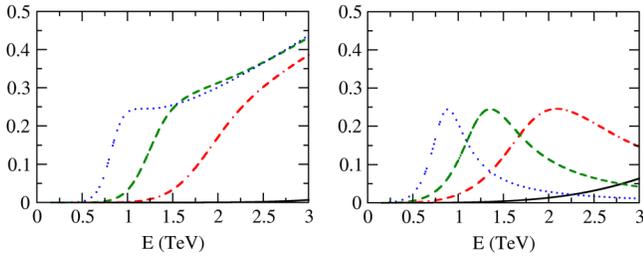
FIG. 3 (color online).   Left graph: Elastic $|A^{IAM}|^2$. Right graph: Cross-channel $|M^{IAM}|^2$. Various values of b shown are $b = 1.1$ (lowest, solid black line), $b = 1.5$ (dot-dashed, red line), $b = 2$ (dashed, green line), and $b = 3$ (dotted, blue line). The inelastic amplitude M^{IAM} shows the resonance with most clarity: it becomes narrower and less massive for larger b.

For larger b, there is a resonant structure most clearly seen in the inelastic process $\omega\omega \to hh$, but that leaves a trace also in the elastic amplitudes that grow almost vertically for large b and even peak slightly up to the resonance mass, growing more calmly afterwards.

In order to explore in more detail the peaks in Fig. 3, we have analytically extended the complex $\log(-s/\mu^2)$ of Eqs. (3)–(5) to the second Riemann sheet, and indeed we found a pole (see Fig. 4) at the same point in all the channels. This pole is naturally interpreted as a dynamical resonance whenever it is close enough to the physical, real s. Then the position of the pole s_0 is related to the parameters of the resonance (mass M and width Γ) as
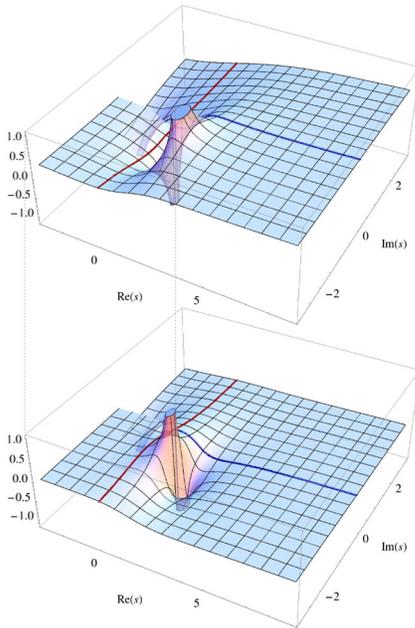

FIG. 4 (color online).   Imaginary part of the unitarized partial waves in the second Riemann sheet in terms of the Mandelstam variable s for $b = 2$. Top: The elastic amplitude A^{IAM}. Bottom: The inelastic amplitude M^{IAM}. These amplitudes are different, but still they show a pole at the same point of the second Riemann sheet that could be understood as a new resonance.
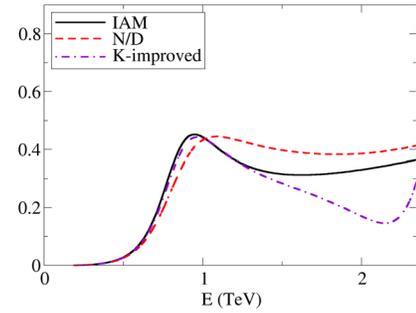

FIG. 5 (color online).   Three unitarization methods closely agree on the existence of a coupled-channel resonance (we show $\mathrm{Im}A = |A|^2 + |M|^2$ for $a \to 1$, $b = 3$). The $I = J = 0$ IAM mass (0.95 TeV) is within 2% of the improved-K and within 10% of the N/D methods.

$s_0 = M^2 - i\Gamma M$, which for small Γ/M means $\sqrt{s_0} \simeq M - i\Gamma/2$. We follow these variables with b in the complex s plane, numerically finding the zeros of the denominator of Eq. (7) in the second Riemann sheet (that denominator is an even function of $b - 1$, so there is an approximate symmetry between $b > 1$ and $b < 1$). The pole escapes to infinity as b approaches 1 and then returns along nearly the same trajectory as b increases beyond 1.

Currently, there is no constraint on the b parameter, but, if a is set to its SM value of 1, and in the absence of NLO couplings, we can provide the bound $b \in (-1, 3)$ (around the SM $b = 1$), because otherwise the resonance moves below 700 GeV, where it would have already been seen by ATLAS and CMS. These exclusion limits on b are, of course, uncertain by $M_W/E \simeq 15\%$ from our using the equivalence theorem ($\omega^a \simeq W^a_L$) and, consistently, the massless Higgs approximation $M_h \ll E$.

Another potential source of uncertainty is the IAM unitarization employed. In the accompanying article, we also address the N/D method and the improved-K matrix. Because the scalar resonance follows from unitarity and analyticity (causality) in the presence of strong channel coupling, all three methods (that encode those properties and agree with perturbation theory at low energy) find it at a very similar position (see Fig. 5).
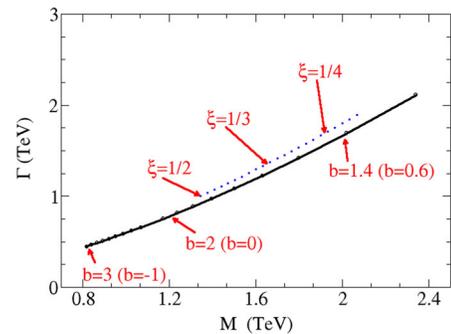

FIG. 6 (color online).   Dependence of resonant mass and width on b, with $a^2 = 1$ fixed (lower curve) and for $a = \sqrt{1 - \xi}$, $b = 1$–2ξ with $\xi = v^2/f^2$ as in the MCHM (upper blue curve).
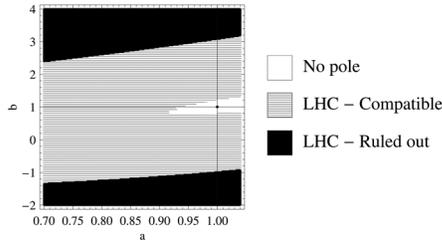
FIG. 7.   Parameter $a - b$ plane showing whether the resonance mass is beyond the 3 TeV reach of our approach (white), below 700 GeV and disfavored by LHC data (black), or between those two values, where we can trust theory and data still allow (striped). The SM value $a = b = 1$ is also marked.

Once we have identified the new coupled-channel resonance by switching off the LO elastic $W_L W_L$ channel by setting $a = 1$, we can consider now the more general case of arbitrary a. From the LHC data, we know this parameter must belong to the 2σ interval (0.88,1.15) (ATLAS) and (0.96,1.34) (CMS) [20], while b is much more unconstrained. As commented above, the simplest composite model where the three ω^a and h show up as composite (pseudo-)GB is the MCHM featuring the symmetry-breaking pattern $SO(5)$ to $SO(4)$ [4]. In this model, the a and b parameters are given by $a = \sqrt{1 - \xi}$ and $b = 1 - 2\xi$, where $\xi = v^2/f^2$ and f is a new symmetry-breaking, higher scale. The relevant IAM partial waves in the general case $a \neq 1$ may be retrieved from Refs. [10,21]. In Fig. 6, we show the mass and width in terms of ξ for the MCHM model. Our new resonance appears for an important range of the allowed ξ parameter range ($0 < \xi < 0.5$). Even for the region where the pole is too far away from the real axis to be considered a resonance, it will produce a huge increment of the cross section for $W_L W_L$ and hh production that could be probed at the LHC. This conclusion probably applies to other composite models beyond the MCHM, too. The figure also shows the pure coupled-channel case $a = 1 \neq b^2$ described above. For finite $a - 1$, the resonance receives strength from both elastic and coupled-channel scattering, but we have shown [13,21] that the σ-like structure from elastic dynamics alone is much broader; for finite $b - a^2$, the resonance, as shown in Fig. 6, is significantly narrower and lighter due to the coupled-channel dynamics. Figure 7 shows the $a - b$ parameter plane showing (with stripes) the region where the resonance in the 2nd Riemann sheet is between 700 GeV and 3 TeV.

In conclusion, we made the case for an interesting potential phenomenon to be sought at LHC run II and beyond, a new resonance in the $W_L W_L - hh$ coupled channels, caused by the channel-mixing interaction even when direct elastic interactions in both channels are weak [22]. We do not have a strong reason to *predict* this resonance but rather observe that it features in the largest part of parameter space of the effective Lagrangian with the known particle content, that supports strong channel coupling. The alternative, weakly coupled resonances that do not saturate unitarity imply parameters fine-tuned to be very close to $a = b = 1$, those of the standard model (that also remains a viable theory with current data).

[1] S. Chatrchyan *et al.* (CMS Collaboration), Phys. Lett. B **716**, 30 (2012); G. Aad *et al.* (ATLAS Collaboration), Phys. Lett. B **716**, 1 (2012).

[2] G. Aad *et al.* (ATLAS Collaboration), Phys. Rev. Lett. **113**, 171801 (2014). Bounds are even higher, well into the TeV region, for new vector resonances; see G. Aad *et al.* (ATLAS Collaboration), Phys. Rev. D **91**, 052007 (2015).

[3] D. B. Kaplan and H. Georgi, Phys. Lett. **136B**, 183 (1984).

[4] K. Agashe, R. Contino, and A. Pomarol, Nucl. Phys. **B719**, 165 (2005); R. Contino, L. Da Rold, and A. Pomarol, Phys. Rev. D **75**, 055014 (2007).

[5] E. Halyo, Mod. Phys. Lett. A **08**, 275 (1993); W. D. Goldberger, B. Grinstein, and W. Skiba, Phys. Rev. Lett. **100**, 111802 (2008).

[6] R. Alonso, M. B. Gavela, L. Merlo, S. Rigolin, and J. Yepes, Phys. Lett. B **722**, 330 (2013).

[7] G. Buchalla, O. Cata, and C. Krause, Nucl. Phys. **B880**, 552 (2014); G. Buchalla and O. Cata, J. High Energy Phys. 07 (2012) 101.

[8] A. Longhitano, Phys. Rev. D **22**, 1166 (1980); Nucl. Phys. **B188**, 118 (1981); A. Dobado, D. Espriu, and M. J. Herrero, Phys. Lett. B **255**, 405 (1991); B. Holdom and J. Terning, Phys. Lett. B **247**, 88 (1990); A. Dobado, D. Espriu, and M. J. Herrero, Phys. Lett. B **255**, 405 (1991); M. Golden and L. Randall, Nucl. Phys. **B361**, 3 (1991).

[9] J. M. Cornwall, D. N. Levin, and G. Tiktopoulos, Phys. Rev. D **10**, 1145 (1974).

[10] R. L. Delgado, A. Dobado, and F. J. Llanes-Estrada, J. High Energy Phys. 02 (2014) 121.

[11] S. Weinberg, Physica (Amsterdam) **96A**, 327 (1979); J. Gasser and H. Leutwyler, Ann. Phys. (N.Y.) **158**, 142 (1984).

[12] R. Contino, C. Grojean, M. Moretti, F. Piccinini, and R. Rattazzi, J. High Energy Phys. 05 (2010) 089.

[13] R. L. Delgado, A. Dobado, and F. J. Llanes-Estrada, J. Phys. G **41**, 025002 (2014).

[14] D. Espriu, F. Mescia, and B. Yencho, Phys. Rev. D **88**, 055002 (2013).

[15] Similar proposals are known in hadron physics, e.g., the $I = 1/2$ resonance oscillating between ϕN and $K^*\Lambda$ around 2 GeV in K. P. Khemchandani, H. Kaneko, H. Nagahiro, and A. Hosaka, Phys. Rev. D **83**, 114041 (2011); see also E. Oset and A. Ramos, Eur. Phys. J. A **44**, 445 (2010).

[16] A. Dobado, M. J. Herrero, and T. N. Truong, Phys. Lett. B **235**, 129 (1990); A. Dobado and J. R. Pelaez, Phys. Rev. D **47**, 4883 (1993); **56**, 3057 (1997).

[17] J. R. Pelaez, J. A. Oller, and E. Oset, Nucl. Phys. **A675**, 92 (2000).

[18] A. Gomez-Nicola and J. R. Pelaez, Phys. Rev. D **65**, 054009 (2002).

[19] D. Espriu and B. Yencho, Phys. Rev. D **87**, 055017 (2013).

[20] CMS Collaboration, Report No. CMS-PASHIG-14-009; ATLAS Collaboration, Report No. ATLAS-CONF-2014-009.

[21] R. L. Delgado, A. Dobado, and F. J. Llanes-Estrada, Phys. Rev. D **91**, 075017 (2015).

[22] Outside particle physics, one can find strongly coupled channels with small elastic interaction. For example, $C_2 + O_2 \rightarrow C_2 + O_2$ or $CO + CO \rightarrow CO + CO$ elastic scattering is negligible against the channel coupling $C_2 + O_2 \rightarrow 2CO$, a strong exothermic oxidation reaction, freeing almost 11 eV, driven by the large phase space. What is perhaps distinctive in our mechanism is that the *channel-coupling probability* is large, with no phase space advantage (all particles being approximately massless).